

Published in final edited form as:

Hepatology. 2013 May ; 57(5): . doi:10.1002/hep.26173.

Endoplasmic reticulum polymers impair luminal protein mobility and sensitise to cellular stress in α_1 -antitrypsin deficiency

Adriana Ordóñez¹, Erik L Snapp², Lu Tan¹, Elena Miranda^{1,3}, Stefan J Marciniak^{1,*}, and David A Lomas^{1,*}

¹Department of Medicine, University of Cambridge, Cambridge Institute for Medical Research, Wellcome Trust/MRC Building, Hills Road, Cambridge CB2 0XY, UK

²Department Anatomy and Structural Biology, Albert Einstein College of Medicine of Yeshiva University, Bronx, NY 10461, USA

³Dipartimento di Biologia e Biotechnologie 'Charles Darwin' e Istituto Pasteur – Fondazione Cenci Bolognetti, Università di Roma "La Sapienza", p.le Aldo Moro 5, 00185 Rome, Italy

Abstract

Point mutants of α_1 -antitrypsin form ordered polymers that are retained as inclusions within the endoplasmic reticulum (ER) of hepatocytes in association with neonatal hepatitis, cirrhosis and hepatocellular carcinoma. These inclusions cause cell damage and predispose to ER stress in the absence of the classical unfolded protein response (UPR). The pathophysiology underlying this ER stress was explored by generating cell models that conditionally express wildtype α_1 -antitrypsin, two mutants that cause polymer-mediated inclusions and liver disease (E342K [the Z allele] and H334D) and a truncated mutant (Null Hong Kong, NHK) that induces classical ER stress and is removed by ER associated degradation. Expression of the polymeric mutants resulted in gross changes in the ER luminal environment that recapitulated the changes seen in liver sections from individuals with PI*ZZ α_1 -antitrypsin deficiency. In contrast expression of NHK α_1 -antitrypsin caused electron lucent dilatation and expansion of the ER throughout the cell. Photobleaching microscopy in live cells demonstrated a decrease in the mobility of soluble luminal proteins in cells that express E342K and H334D α_1 -antitrypsin when compared to those that express wildtype and NHK α_1 -antitrypsin (0.34 ± 0.05 , 0.22 ± 0.03 , 2.83 ± 0.30 and 2.84 ± 0.55 $\mu\text{m}^2/\text{s}$ respectively). There was no effect on protein mobility within ER membranes indicating that cisternal connectivity was not disrupted. Polymer expression alone was insufficient to induce the UPR but the resulting protein overload rendered cells hypersensitive to ER stress induced by either tunicamycin or glucose depletion.

Conclusion—Changes in protein diffusion provide an explanation for the cellular consequences of ER protein overload in mutants that cause inclusion body formation and α_1 -antitrypsin deficiency.

Keywords

cirrhosis; serpins; UPR; diffusion; FRAP-FLIP

Corresponding Author: Dr Stefan J Marciniak, Department of Medicine, University of Cambridge, Cambridge Institute for Medical Research, Wellcome Trust/MRC Building, Hills Road, Cambridge, CB2 0XY, UK, sjm20@cam.ac.uk; Tel: +44 (0)1223 762660; Fax: +44 (0)1223 336827.

*Joint senior authors

The authors declare no conflict of interest. SJM, DAL, AO and EM designed the project. AO, ELS and LT carried out the experiments and data analysis. All authors participated in writing the manuscript.

Introduction

Alpha₁-antitrypsin deficiency results from point mutations that lead to the formation of large, ordered polymers that accumulate within the ER of hepatocytes¹. The resulting inclusions cause a toxic-gain-of-function that is associated with neonatal hepatitis, cirrhosis and hepatocellular carcinoma². This is best exemplified by the Z (E342K), King's (H334D), Siiyama (S53F) and Mmalton (Δ 52F) alleles³⁻⁶. Plasma efficiency of α_1 -antitrypsin deficiency can also result from truncating mutations such as the Null Hong Kong (NHK) allele that target the protein for ER-associated degradation (ERAD)⁷. This reduces secretion of α_1 -antitrypsin but does not cause the gain-of-function liver disease. In both cases the lack of circulating α_1 -antitrypsin predisposes the homozygote to early onset emphysema⁸.

A wide range of signalling pathways are activated to restore the ER homeostasis in response to an overload of misfolded proteins. An important stress response is the Unfolded Protein Response (UPR) that combines transient attenuation of protein translation with enhancement of the ER's protein-folding capacity, thus preventing uncontrolled aggregation of proteins within its lumen⁹. This conserved stress response is tightly regulated by the activation of three ER stress sensors operating in parallel: IRE1, PERK, and ATF6. Under non-stressed conditions, each sensor is held in an inactive state by binding of the ER chaperone BiP to its luminal domain. When misfolded protein levels increase during ER stress, the UPR is activated, at least in part, through the titration of BiP away from these sensor molecules.

We aimed to determine the impact of polymers and truncated α_1 -antitrypsin on the ER environment. We show that the accumulation of ordered polymers of α_1 -antitrypsin leads to gross expansion of ER cisternae and impairment of ER luminal mobility. This hinders the organelle's capacity to deal with otherwise minor perturbations of protein folding and thus leads to enhanced sensitivity to ER stress. Our findings provide one of several potential mechanisms for the toxicity associated with ER overload in α_1 -antitrypsin deficiency related liver disease.

Material and Methods

Plasmid constructs

cDNA for human wildtype α_1 -antitrypsin and two polymeric mutants (E342K and H334D) were subcloned into the pTRE2hyg vector (Clontech) for the generation of stable CHO-K1 Tet-On α_1 -antitrypsin cell lines. The NHK truncated α_1 -antitrypsin variant (L318fsX17) was generated with the QuickChange™ Site-Directed Mutagenesis kit (Stratagene) using wildtype α_1 -antitrypsin as the template and then subcloned into the pTRE2hyg plasmid.

Generation and characterization of stable cell lines expressing α_1 -antitrypsin

The CHO-K1 cell line was purchased from Clontech and stable cell lines were generated by following the manufacturer's instructions. The cells were maintained in DMEM supplemented with 10% v/v Tet-FBS, 1% w/v non-essential amino acids, 1% w/v penicillin/streptomycin, 200 μ g/ml Geneticin, and 500 μ g/ml Hygromycin B (both selective antibiotics from Invitrogen) at 37°C and 5% v/v CO₂. α_1 -Antitrypsin was typically induced with 1 μ g/ml doxycycline for 48h. Whole cell lysates, SDS and non-denaturing polyacrylamide gel electrophoresis (PAGE) followed by immunoblotting, ELISA analysis and metabolic labelling were performed as detailed previously^{4,10} (see Supporting Materials and Methods).

Immunofluorescence, electron microscopy and immunocytochemistry

Immuno- and electron microscopy of CHO-K1 cells and immunocytochemistry of paraffin tissue slides from human subjects were undertaken as described in the Supporting Materials and Methods.

Photobleaching analysis in live cells

CHO-K1 Tet-On cells were transiently transfected with an ER-RFP plasmid¹¹ or a CytERM msfGFP membrane reporter¹². Live cells were imaged on a 37°C environmental controlled stage of a confocal microscope system (Duoscan; Carl Zeiss Inc.) with a 63x/1.4NA oil objective and a 40 mW 561nm diode laser with a 565nm bandpass filter. For FRAP/FLIP experiments, a small region of interest was photobleached at full laser power in the 561 line and fluorescence recovery or loss was monitored over 0.2s time intervals. Diffusion (D_{eff}) measurements were calculated as described previously¹³. Fluorescence loss curves were obtained by transforming the fluorescence intensities into a percentage scale in which the first bleach time point represents 100% of fluorescence intensity. Statistical significance was assessed using Student's t test.

Detection of the UPR markers

Immunoblots for three main ER luminal chaperone proteins (GRP94, BiP/GRP78, PDI), the ATF6-reporter luciferase assay and the RT-PCR XBP1 splicing assay were performed as described previously¹⁰.

Results

Conditional expression of α_1 -antitrypsin

Stable CHO-K1 cell lines were developed using the Tetracycline-On (Tet-On) inducible system that enables tight regulation of α_1 -antitrypsin expression. Four clonal cell lines were generated to express four single variants of α_1 -antitrypsin: the wildtype human α_1 -antitrypsin (M); the polymeric Z [E342K] mutant; the polymeric King's [H334D] mutant (both form ordered polymers in the ER of hepatocytes in association with liver disease^{3,4}); and a NHK truncated variant that does not fold properly, preventing the formation of ordered polymers, and instead activates the UPR⁷. Expression of each variant was readily detected on treating cells with doxycycline (Figs. 1 and S1A–E). Cells expressing M α_1 -antitrypsin showed lower intracellular signal compared to medium, consistent with its efficient secretion. Non-denaturing PAGE and ELISA assays identified intracellular polymers for only Z and H334D α_1 -antitrypsin. No ELISA signal was detected for the NHK variant, suggesting that the 9C5 epitope that is present in monomeric and polymeric forms of α_1 -antitrypsin, was removed by the deletion of the C-terminal 61 amino acids. Protein trafficking rate was assayed by metabolic labeling followed by immunoprecipitation (Fig. 1C). Wildtype α_1 -antitrypsin was almost completely secreted, compared with Z and H334D α_1 -antitrypsin, which were largely retained as polymers. In contrast, NHK α_1 -antitrypsin failed to reach the culture medium despite being cleared from the cell lysates at 4h, consistent with its degradation by ER associated degradation (ERAD)⁷.

Accumulation of α_1 -antitrypsin polymers causes disruption of the ER

Immunofluorescence confocal microscopy revealed that both Z and H334D α_1 -antitrypsin co-localised with the ER marker BiP, although in many cells the ER structure was distorted from its reticular morphology into a punctate pattern (Fig. 2A). No gross morphological changes were observed in cells expressing either M or NHK α_1 -antitrypsin. Of note, only M α_1 -antitrypsin co-localised with the Golgi marker p115, indicating efficient exit from the ER (Fig. 2A). Electron microscopy was used to visualise cells expressing wildtype and mutant

α_1 -antitrypsin. The ultrastructure in cells expressing M α_1 -antitrypsin was normal (Fig. 2B; a–b) when they were compared with mock-transfected cells (Fig. 2B; i–k). The inclusions in cells expressing either Z or H334D α_1 -antitrypsin were associated with the replacement of normal tubular and lamellar ER by electron-dense vesiculated structures (Fig. 2B; c–f). In contrast, expression of the NHK variant induced a markedly different phenotype with electron lucent dilatation and expansion of the ER throughout the cell (Fig. 2B; g–h). In order to elucidate whether the alterations observed could be due to a massive overexpression of α_1 -antitrypsin in our model, we also assessed the distribution and signal of total α_1 -antitrypsin in paraffin-embedded liver sections from a PI*ZZ α_1 -antitrypsin homozygote and control human liver by immunocytochemistry (Fig. 2C). The PI*ZZ homozygote human liver demonstrated levels of polymer accumulation at least as dramatic as that seen in cultured cells, suggesting that the CHO-K1 Tet-On cells represent a valid model of the accumulation of α_1 -antitrypsin polymers within the ER. Taken together, these data show that the accumulation of ordered polymers within the ER leads to gross changes in the organelle's morphology and importantly that these changes differ markedly from those induced by the NHK mutant that causes classical ER stress.

Polymeric mutants of α_1 -antitrypsin impair ER protein mobility in live cells

The impact of polymer formation on the ER luminal environment was determined by monitoring changes in the mobility of the ER-RFP fluorescence marker in live cells. ER-localised RFP is a protein (27kDa and 2.3 nm hydrodynamic radius) with no known interacting partners that can rapidly sample the entire ER lumen, reporting on both crowdedness and interconnectivity¹¹. The ER-RFP distribution revealed two distinct ER architectures in cells expressing α_1 -antitrypsin variants. Each cell line displayed a typical ER reticular network in the absence of doxycycline, as did cells expressing M and NHK α_1 -antitrypsin when treated with doxycycline (Fig. S2). In contrast, approximately 30–40% of cells expressing Z and H334D α_1 -antitrypsin developed a characteristic vesiculated architecture when treated with doxycycline (Fig. S2), as detected by staining for either α_1 -antitrypsin or BiP (Fig. 2A). Within the same clonal cell lines there remained a proportion of cells expressing Z and H334D α_1 -antitrypsin that retained the normal reticular pattern of ER, suggesting that formation of inclusion bodies is a stochastic phenomenon (Fig. S3).

We then assessed the ER lumen continuity by fluorescence loss in photobleaching (FLIP)¹⁴, in which a small region of the cell ER-RFP fluorescence was repeatedly photobleached. If the protein is mobile within a continuous compartment, the total fluorescence within this compartment will be depleted. Over time, ER-RFP fluorescence in the whole cell was steadily and uniformly lost in cells displaying a tubular ER network, whereas fluorescence depletion was substantially slower in cells containing Z α_1 -antitrypsin polymer (Fig. 3A and Movies S1 and S2). This did not reflect an effect of transfected ER-RFP expression levels, since normalised plots showed that the remaining whole cell fluorescence intensity after 200 s was 23.5% and 61.1% for cells retaining a tubular ER network or a polymer-filled ER, respectively (Fig. 3A). Similar results were obtained for cells expressing H334D α_1 -antitrypsin (Fig. 3B). Thus, the presence of vesiculated structures is associated with marked loss of intra-ER luminal communication (slower ER-RFP mobility between inclusions) that is likely to adversely increase the heterogeneity of the ER luminal environment.

FRAP analysis was used to quantify the change in mobility of the ER-RFP reporter (Fig. 4A). This provides information on local rates of protein diffusion, D_{eff} ($\mu\text{m}^2/\text{s}$) by bleaching a small defined region of a single cell. D_{eff} is affected by local viscosity, size of the reporter protein and its protein-protein interactions¹⁵ and is inversely proportional to crowdedness of the environment. Moreover, small changes in D_{eff} are likely to be biologically significant¹¹. No significant differences in the mobility of ER-RFP were detected in the different cell lines

in the absence of α_1 -antitrypsin expression (Fig. 4B). ER-RFP D_{eff} values in cells expressing NHK and M α_1 -antitrypsin were identical (2.84 ± 0.30 vs. $2.83 \pm 0.55 \mu\text{m}^2/\text{s}$). However, cells containing polymers of either Z or H334D α_1 -antitrypsin exhibited significantly lower ER-RFP D_{eff} values compared with M α_1 -antitrypsin (0.34 ± 0.05 and $0.22 \pm 0.03 \mu\text{m}^2/\text{s}$ respectively; Figs. 4A and B, and Movies S2 and S3).

The striking effect of polymers on the ER-RFP diffusion within the lumen of the ER, prompted an assessment of their effect on the diffusion of an ER transmembrane reporter. We used the CytERM msfGFP plasmid, which encodes a signal domain required to anchor the fluorescent protein into the ER membrane with the sfGFP exposed to the cytoplasm¹². There is no luminal domain and consequently the luminal content has no effect on membrane protein diffusion. There were no significant differences in CytERM msfGFP D_{eff} values in cells containing polymers of H334D α_1 -antitrypsin compared to cells in which expression was not induced (0.35 ± 0.04 vs. $0.40 \pm 0.02 \mu\text{m}^2/\text{s}$) (Fig. 4C).

Taken together, these data demonstrate that inclusions of α_1 -antitrypsin polymers have a remarkable effect on the ER environment reducing luminal protein diffusion. However protein mobility within ER membranes is unaffected, indicating that cisternae connectivity is not disrupted.

Increased susceptibility to ER stress in polymer expressing cells

Previous work has shown that the ER accumulation of ordered polymers of mutant α_1 -antitrypsin and another member of the same protein family, neuroserpin, fail to activate the UPR^{16–19}. However, a recent report has suggested that Z α_1 -antitrypsin polymer accumulation triggers UPR activation in peripheral blood monocytes²⁰. We hypothesised that the alteration of the ER luminal environment might destabilise ER homeostasis sufficiently to sensitise the cell to a second insult and so trigger activation of the UPR. The activation of multiple reporters of UPR signalling was monitored following treatment with tunicamycin, an inhibitor of N-linked glycosylation. Immunoblot analysis for three ER luminal chaperones (BiP/GRP78, GRP94 and PDI) confirmed that ordered polymers of α_1 -antitrypsin alone failed to activate the UPR (Fig. 5A; lanes 1–3). In contrast and as expected, synthesis of the truncated NHK α_1 -antitrypsin led to robust activation of the UPR (Fig. 5A; lane 4). Remarkably, both polymerogenic α_1 -antitrypsin variants showed a hypersensitive response in UPR activation following treatment with low concentrations of tunicamycin (5–25 ng/ml) when compared to the wildtype protein (Fig. 5A).

A more quantitative reporter assay was used to assess the activation of the ATF6 branch of the UPR. Only cells expressing NHK α_1 -antitrypsin showed measureable activation of ATF6 under non-stressed conditions (Fig. 5B). However cells expressing polymeric variants were more susceptible to activation of ATF6 on treatment with moderate concentrations of tunicamycin (60–300 ng/ml). A similar response was seen when cells were treated with low concentrations of glucose (10–0.2 mM), which represents a more physiological ER stress (Fig. 5C).

IRE1 activation was assessed by the splicing of *XBPI* mRNA. None of the cell lines showed spliced *XBPI* mRNA under basal conditions. However, tunicamycin (300 ng/ml) efficiently triggered IRE1 in all cell lines as reported by the appearance of a smaller spliced *XBPI* mRNA band (Fig. 5D). The failure to detect splicing of *XBPI* mRNA in cells induced to express the NHK variant in the absence of tunicamycin reflects the transitory nature of IRE1 activation²¹. Following the induction of ER chaperones, which occurs rapidly on expressing this truncated mutant, ER stress is alleviated and IRE1 returns to its inactive state. Indeed, the elevated level of ER chaperones in NHK-expressing cells served to protect them from subsequent ER stress, as evidenced by the blunted response of *XBPI* splicing seen in these

cells (Fig. 5D). In contrast, on treatment with tunicamycin, M, Z- and H334D-expressing cells showed rapid splicing of *XBP1* mRNA. These data indicate that the presence of polymers does not affect the intrinsic activity of IRE1. They do, however, impair the cell's ability to restore ER homeostasis, since higher levels of spliced *XBP1* mRNA persisted after 16h treatment with tunicamycin in cells expressing both Z and H334D α_1 -antitrypsin compared to the wildtype protein.

It is possible that differences in the sensitivity to tunicamycin might be responsible for the enhanced UPR activation in cells that express polymers of α_1 -antitrypsin. However this was not the case as treatment with tunicamycin resulted in equal levels of a slower migrating glycosylated form of α_1 -antitrypsin and a faster migrating non-glycosylated form in each α_1 -antitrypsin expressing cell line (Fig. S4).

Discussion

It is well recognised that point mutations of α_1 -antitrypsin form ordered polymers that are retained as inclusions within the ER, resulting in ER dysfunction and liver disease⁸. These inclusions form in the face of effective disposal of misfolded monomer and polymers by ERAD^{18,22} and autophagy²³. One of the cellular consequence of the accumulation of these ordered polymers is the ER overload response (EOR), which results in the release of ER calcium and the activation of NF- κ B, a central mediator of inflammation^{19,24}. This pathway is distinct from the canonical UPR, which is triggered by the accumulation of misfolded protein and results in the inhibition of protein synthesis, induction of ER chaperones and ER stress²⁵. The ER overload response and UPR pathways often occur together but mutants of α_1 -antitrypsin provide ideal tools to probe these pathways as the polymer forming mutants activate only the EOR¹⁶⁻¹⁹, whilst truncated mutants activate only the UPR⁷.

We have used two polymeric mutants of α_1 -antitrypsin (E342K and H334D) to determine the mechanism by which ER overload can impact on the organization of the ER environment and the cell's susceptibility to ER stress. Our data reveal that polymers of α_1 -antitrypsin accumulate in spherical, apparently vesiculated ER, concomitantly with loss of the normal branching tubule network. Similar ER vesiculation has been reported to be associated with other cellular stresses, including mechanical injury and elevated cytosolic calcium concentration, although the physiological relevance of this remains unclear^{26,27}. Live-cell imaging revealed that accumulation of polymers in vesiculated ER leads to a marked and specific impairment of luminal protein mobility due to an increased ER heterogeneity, which might reflect a change in either the luminal viscosity and/or in the tortuosity for ER-RFP diffusion within and between spherical inclusions. Interestingly, the truncated NHK mutant that causes classical ER stress (UPR) and is efficiently degraded by the proteasome showed a different ultrastructural change characterised by gross expansion of ER cisternae. This had no effect on luminal protein mobility. Current technology limits the area of photobleaching to slightly larger than the size of an inclusion. However, since effects of photobleaching were examined by FLIP throughout the cell, we are confident in these findings. It will be valuable, when the technology has improved sufficiently, to revisit the diffusion between individual inclusions.

In agreement with previous studies¹⁶⁻¹⁹, we report that cells expressing polymers of either Z or H334D α_1 -antitrypsin do not show constitutive activation of the UPR. However these cells do exhibit a hypersensitivity to both pharmacological and physiological ER stressors. To date, most studies that have attempted to detect ER stress in cells expressing mutant α_1 -antitrypsin have made use of methods such as the up-regulation of ER chaperones. Although providing important insights, such approaches have been unable to address how ER overload with polymers of α_1 -antitrypsin might impact on the molecular organization of the ER

organelle. Our observation that enhanced sensitivity to ER stress following the expression of polymerogenic α_1 -antitrypsin mutants correlates with the presence of marked changes in the biophysical features of the ER suggests a mechanism for this phenomenon (Fig. 6). Chaperones can readily diffuse to sites of protein misfolding in cells possessing a reticular and highly interconnected ER. In contrast, in cells experiencing ER overload, a comparable level of misfolded client protein cannot diffuse freely, decreasing their accessibility to quality control proteins required for folding and transport. Therefore, we propose a model in which decreased mobility or availability of ER chaperones due to changes in the diffusive features or/and obstruction caused by protein overload, sensitises the cell to subsequent activation of the UPR by a second hit that further increases the unfolded secretory protein burden. Our findings are directly relevant to the liver disease associated with polymerogenic mutants of α_1 -antitrypsin. However, although polymer accumulation involves a gain-of-function associated with liver dysfunction, epidemiological studies have shown that only 10% of patients with α_1 -antitrypsin deficiency develop clinically apparent liver disease²⁸. It appears that additional, incompletely understood genetic and environmental factors contribute to this heterogeneity in hepatic phenotype^{29,30}. Our results suggest that polymer accumulation increases the vulnerability of the cell to a ‘second hit’ that ultimately initiates liver disease in individuals with α_1 -antitrypsin deficiency. Moreover, the mechanism proposed is likely to be relevant to other serpinopathies, such as the neuronal toxicity associated with polymers of neuroserpin in the dementia FENIB³¹.

Supplementary Material

Refer to Web version on PubMed Central for supplementary material.

Acknowledgments

This work was supported by the postdoctoral fellowship grant from the eALTA Foundation (Griffols) to AO. SJM is an MRC Senior Clinical Fellow (G0601840). ELS is supported by NIGMS R01GM086530–01. DAL is supported by the Medical Research Council (UK), the Cambridge NIHR Biomedical Research Centre, the Engineering and Physical Sciences Research Council (UK) and Papworth NHS Trust. LT is supported by the NIHR Biomedical Research Centre and the British Research Council. EM is supported by the Istituto Pasteur-Fondazione Cenci Bolognetti and by the Telethon Foundation, Italy. The authors thank Marianna Mela, Department of Medicine, University of Cambridge for providing the human liver tissue and Dr James Irving for his help preparing the figures and movies.

Abbreviations

α1AT	α_1 -antitrypsin
D_{eff}	Effective diffusion coefficient
Dox	Doxycycline
EOR	Endoplasmic overload response
ER	Endoplasmic reticulum
FLIP	Fluorescence loss in photobleaching
FRAP	Fluorescence recovery after photobleaching
Tm	Tunicamycin
UPR	Unfolded protein response

References

1. Lomas DA, Carrell RW. Serpinopathies and the conformational dementias. *Nat Rev Genet.* 2002; 3:759–768. [PubMed: 12360234]
2. Wu Y, Whitman I, Molmenti E, Moore K, Hippenmeyer P, Perlmutter DH. A lag in intracellular degradation of mutant alpha 1-antitrypsin correlates with the liver disease phenotype in homozygous PiZZ alpha 1-antitrypsin deficiency. *Proc Natl Acad Sci USA.* 1994; 91:9014–9018. [PubMed: 8090762]
3. Lomas DA, Evans DL, Finch JT, Carrell RW. The mechanism of Z alpha 1-antitrypsin accumulation in the liver. *Nature.* 1992; 357:605–607. [PubMed: 1608473]
4. Miranda E, Pérez J, Ekeowa UI, Hadzic N, Kalsheker N, Gooptu B, Portmann B, et al. A novel monoclonal antibody to characterize pathogenic polymers in liver disease associated with alpha1-antitrypsin deficiency. *Hepatology.* 2010; 52:1078–1088. [PubMed: 20583215]
5. Lomas DA, Finch JT, Seyama K, Nukiwa T, Carrell RW. Alpha 1-antitrypsin Siiyama (Ser53-->Phe). Further evidence for intracellular loop-sheet polymerization. *J Biol Chem.* 1993; 268:15333–15335. [PubMed: 8340361]
6. Lomas DA, Elliott PR, Sidhar SK, Foreman RC, Finch JT, Cox DW, Whisstock JC, et al. alpha 1-Antitrypsin Mmalton (Phe52-deleted) forms loop-sheet polymers in vivo. Evidence for the C sheet mechanism of polymerization. *J Biol Chem.* 1995; 270:16864–16870. [PubMed: 7622502]
7. Sifers RN, Brashears-Macatee S, Kidd VJ, Muensch H, Woo SL. A frameshift mutation results in a truncated alpha 1-antitrypsin that is retained within the rough endoplasmic reticulum. *J Biol Chem.* 1988; 263:7330–7335. [PubMed: 3259232]
8. Gooptu B, Lomas DA. Polymers and inflammation: disease mechanisms of the serpinopathies. *J Exp Med.* 2008; 205:1529–1534. [PubMed: 18591408]
9. Marciniak SJ, Ron D. Endoplasmic reticulum stress signaling in disease. *Physiol Rev.* 2006; 86:1133–1149. [PubMed: 17015486]
10. Irving JA, Ekeowa UI, Belorgey D, Haq I, Gooptu B, Miranda E, Perez J, et al. The serpinopathies studying serpin polymerization in vivo. *Methods Enzymol.* 2011; 501:421–466. [PubMed: 22078544]
11. Snapp EL, Sharma A, Lippincott-Schwartz J, Hegde RS. Monitoring chaperone engagement of substrates in the endoplasmic reticulum of live cells. *Proc Natl Acad Sci US A.* 2006; 103:6536–6541.
12. Costantini LM, Fossati M, Francolini M, Snapp EL. Assessing the Tendency of Fluorescent Proteins to Oligomerize Under Physiologic Conditions. *Traffic.* 2012; 13:643–9. [PubMed: 22289035]
13. Snapp EL. Fluorescent proteins: a cell biologist's user guide. *Trends Cell Biol.* 2009; 19:649–655. [PubMed: 19819147]
14. Snapp EL, Altan N, Lippincott-Schwartz J. Measuring protein mobility by photobleaching GFP chimeras in living cells. *Curr Protoc Cell Biol.* 2003; Chapter 21(Unit)
15. Lippincott-Schwartz J, Snapp E, Kenworthy A. Studying protein dynamics in living cells. *Nat Rev Mol Cell Biol.* 2001; 2:444–456. [PubMed: 11389468]
16. Graham KS, Le A, Sifers RN. Accumulation of the insoluble PiZ variant of human alpha 1-antitrypsin within the hepatic endoplasmic reticulum does not elevate the steady-state level of grp78/BiP. *J Biol Chem.* 1990; 265:20463–20468. [PubMed: 2122976]
17. Hidvegi T, Schmidt BZ, Hale P, Perlmutter DH. Accumulation of mutant alpha1-antitrypsin Z in the endoplasmic reticulum activates caspases-4 and -12, NFkappaB, and BAP31 but not the unfolded protein response. *J Biol Chem.* 2005; 280:39002–39015. [PubMed: 16183649]
18. Kroeger H, Miranda E, MacLeod I, Pérez J, Crowther DC, Marciniak SJ, Lomas DA. Endoplasmic reticulum-associated degradation (ERAD) and autophagy cooperate to degrade polymerogenic mutant serpins. *J Biol Chem.* 2009; 284:22793–22802. [PubMed: 19549782]
19. Davies MJ, Miranda E, Roussel BD, Kaufman RJ, Marciniak SJ, Lomas DA. Neuroserpin polymers activate NF-kappaB by a calcium signaling pathway that is independent of the unfolded protein response. *J Biol Chem.* 2009; 284:18202–18209. [PubMed: 19423713]

20. Carroll TP, Greene CM, O'Connor CA, Nolan AM, O'Neill SJ, McElvaney NG. Evidence for unfolded protein response activation in monocytes from individuals with alpha-1 antitrypsin deficiency. *J Immunol.* 2010; 184:4538–4546. [PubMed: 20228200]
21. Marciniak SJ, Yun CY, Oyadomari S, Novoa I, Zhang Y, Jungreis R, Nagata K, et al. CHOP induces death by promoting protein synthesis and oxidation in the stressed endoplasmic reticulum. *Genes Dev.* 2004; 18:3066–3077. [PubMed: 15601821]
22. Teckman JH, Burrows J, Hidvegi T, Schmidt B, Hale PD, Perlmutter DH. The proteasome participates in degradation of mutant alpha 1-antitrypsin Z in the endoplasmic reticulum of hepatoma-derived hepatocytes. *J Biol Chem.* 2001; 276:44865–44872. [PubMed: 11577074]
23. Hidvegi T, Ewing M, Hale P, Dippold C, Beckett C, Kemp C, Maurice N, et al. An autophagy-enhancing drug promotes degradation of mutant alpha1-antitrypsin Z and reduces hepatic fibrosis. *Science.* 2010; 329:229–232. [PubMed: 20522742]
24. Pahl HL, Baeuerle PA. The ER-overload response: activation of NF-kappa B. *Trends Biochem Sci.* 1997; 22:63–67. [PubMed: 9048485]
25. Kaufman RJ. Orchestrating the unfolded protein response in health and disease. *J Clin Invest.* 2002; 110:1389–1398. [PubMed: 12438434]
26. Raeymaekers L, Lariviere E. Vesicularization of the endoplasmic reticulum is a fast response to plasma membrane injury. *Biochem Biophys Res Commun.* 2011; 414:246–251. [PubMed: 21951855]
27. Subramanian K, Meyer T. Calcium-induced restructuring of nuclear envelope and endoplasmic reticulum calcium stores. *Cell.* 1997; 89:963–971. [PubMed: 9200614]
28. Sveger T. The natural history of liver disease in alpha1-antitrypsin deficient children. *Acta Paediatr Scand.* 1995; 77:847–851. [PubMed: 2905108]
29. Pan S, Huang L, McPherson J, Muzny D, Rouhani F, Brantly M, Gibbs R, et al. *Hepatology.* 2009; 50:275–81. [PubMed: 19444872]
30. Perlmutter DH. Liver injury in 1-antitrypsin deficiency: an aggregated protein induces mitochondrial injury. *J Clin Invest.* 2002; 110:579–1583.
31. Davis RL, Shrimpton AE, Holohan PD, Bradshaw C, Feiglin D, Collins GH, Sonderegger P, et al. Familial dementia caused by polymerization of mutant neuroserpin. *Nature.* 1999; 401:376–379. [PubMed: 10517635]

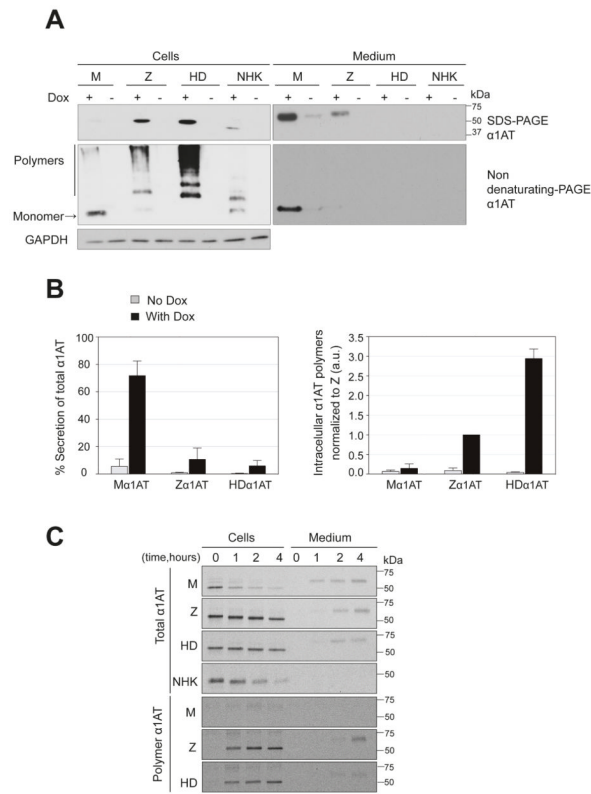


Fig. 1. Characterisation of CHO-K1 Tet-On cell lines expressing different variants of α_1 -antitrypsin (α_1 AT): wildtype (M), Z (E342K), HD (H334D) and the truncated Null Hong Kong (NHK) variant

A) Cell lysates and medium were collected after induction of α_1 -antitrypsin with 1 μ g/ml doxycycline (dox) for 48h and analysed by 10% w/v SDS and non-denaturing PAGE followed by immunoblot for α_1 -antitrypsin. B) Percentage of secreted total α_1 -antitrypsin and quantification of intracellular polymers for M, Z and HD α_1 -antitrypsin were quantified by sandwich ELISA using the 9C5 (left panel) or 2C1 (right panel) monoclonal antibodies, that recognise all forms of α_1 -antitrypsin or only polymers, respectively. The graphs show mean \pm SEM (n=4). C) CHO-K1 Tet-On cells expressing M, Z, HD and NHK α_1 -antitrypsin were pulse-labeled with 35 S-Met/Cys for 15min and chased for the times indicated (0 – 4h). α_1 -Antitrypsin from cell lysates and medium was immunoprecipitated with a polyclonal antibody (total) or the 2C1 monoclonal antibody (polymers) and then samples were resolved by 10% w/v SDS PAGE and detected by autoradiography. Gels are representative of three independent experiments.

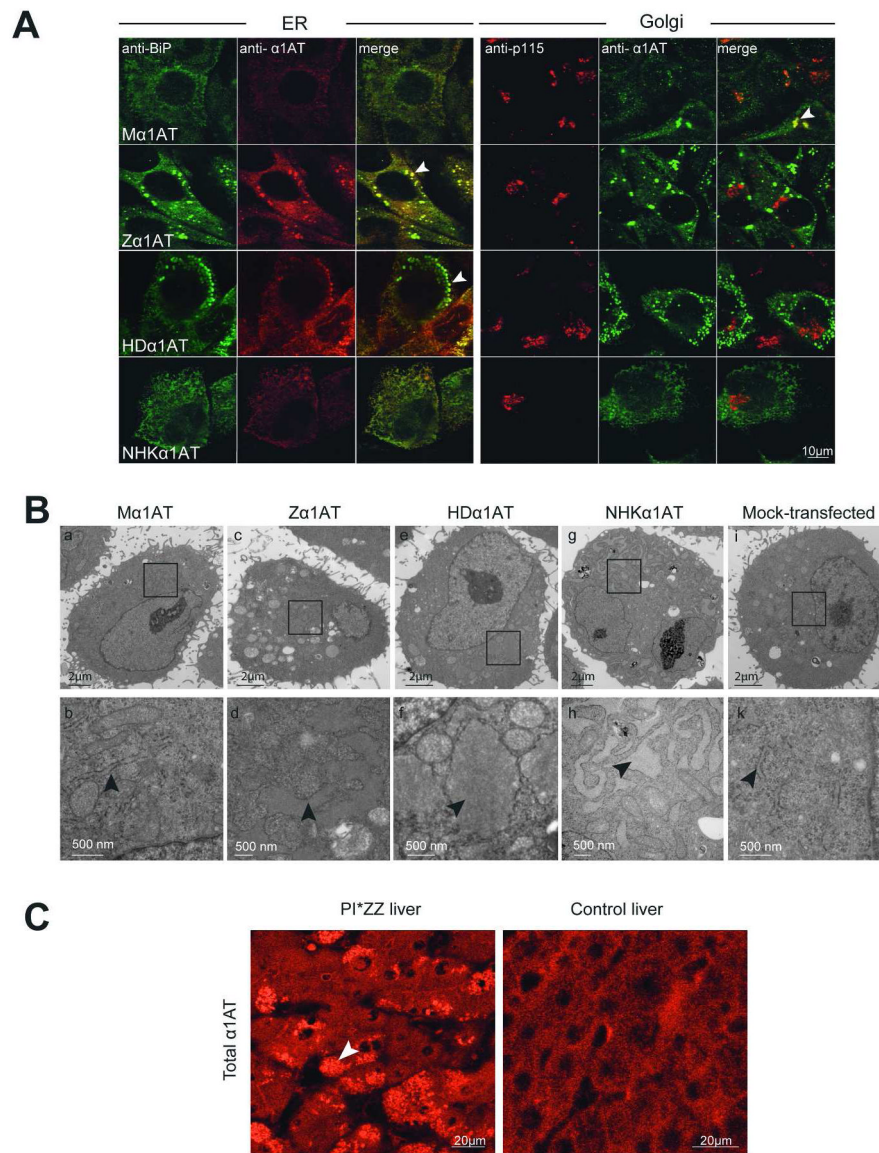


Fig. 2. Intracellular accumulation of α ₁-antitrypsin polymers in inclusion bodies disrupts ER structure

A) Representative fluorescence images of Tet-On CHO-K1 cells induced to express M, Z, HD and NHK α ₁-antitrypsin with dox for 48h, fixed and co-immunostained with an α ₁-antitrypsin polyclonal antibody and either an ER protein marker (BiP) or a Golgi protein marker (p115). White arrows in the merge panels show a punctate pattern of co-localised polymerogenic forms of α ₁-antitrypsin (Z and HD) with the ER marker (left panel) or wildtype α ₁-antitrypsin co-localised with the Golgi marker (right panel). B) Electron microscopy analysis for ER structure in Tet-On CHO-K1 cells expressing α ₁-antitrypsin variants. Upper panels represent whole cells, with higher power images shown in lower panels. Black arrows indicate the ER cisterns. Inclusion bodies were only identified in micrographs of the polymerogenic mutants (Z and HD α ₁-antitrypsin). C) Immunostaining of paraffin-embedded liver sections from a PI*ZZ α ₁-antitrypsin individual and a normal control liver with a polyclonal antibody to total α ₁-antitrypsin (white arrow).

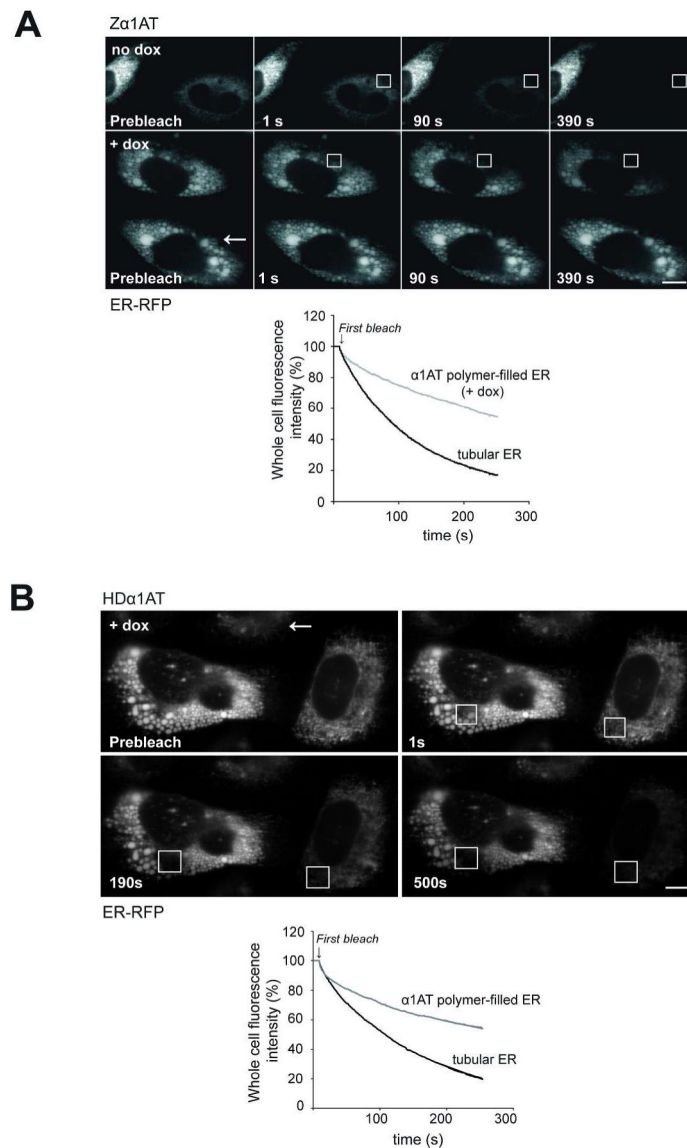


Fig. 3. Luminal α_1 -antitrypsin inclusion bodies impair protein mobility within the ER lumen
 A) FLIP analysis of Z α_1 -antitrypsin cells expressing ER-RFP within both a tubular ER network cell (without dox) and an α_1 -antitrypsin polymer-filled ER (with dox for 48h). FLIP normalised plots setting the pre-bleach intensity as 100%. B) FLIP of H334D α_1 -antitrypsin cells expressing ER-RFP within both a tubular ER network cell and an α_1 -antitrypsin polymer-filled ER from the same sample after treatment with dox for 48h. Normalised plots from FLIP analysis as described in 3A. Fluorescence loss was specific, as adjacent cells remained fluorescent (white arrow). White boxes represent the region subjected to photobleaching.

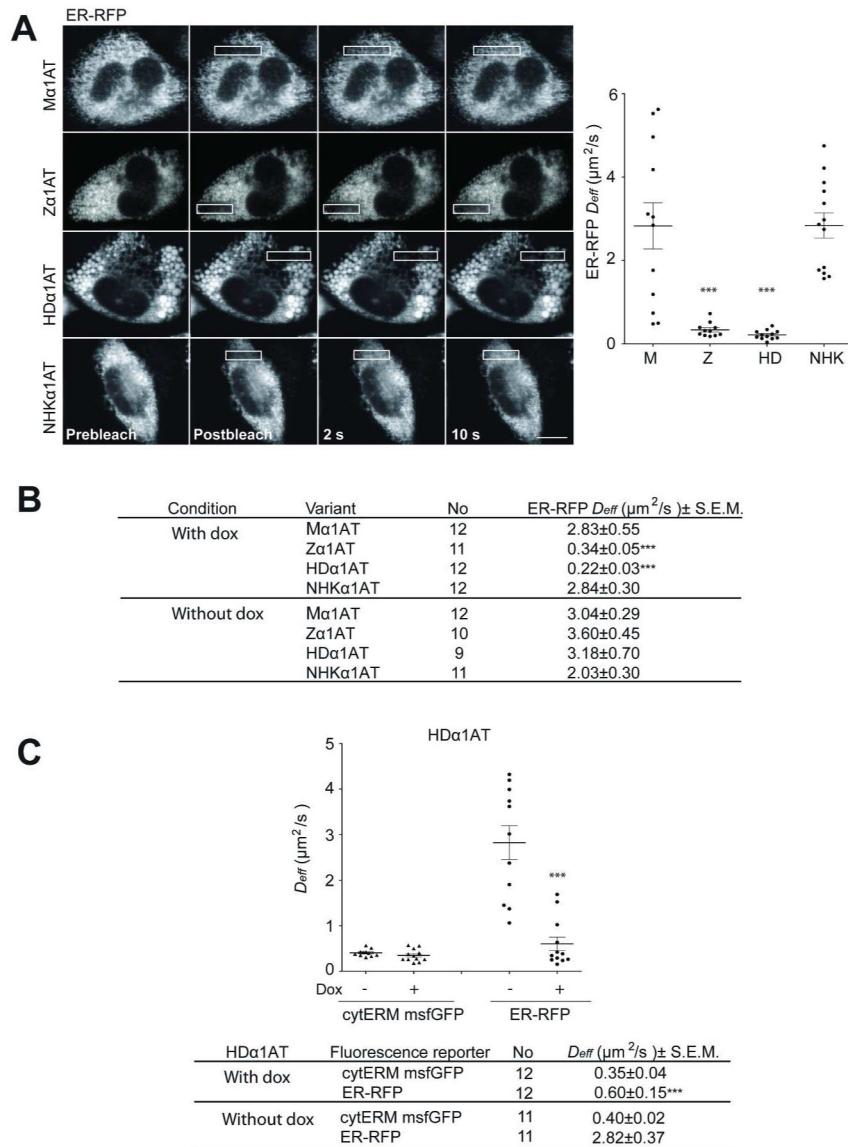


Fig. 4. Polymers of α_1 -antitrypsin modify the ER luminal environment decreasing ER protein mobility

A) Left: FRAP series of Tet-On CHO-K1 cells induced to express M, Z, HD and NHK α_1 -antitrypsin with dox for 48h and transiently co-transfected with ER-RFP. Cells expressing either Z or HD α_1 -antitrypsin show a vesiculated pattern in which the fluorescence recovery was significantly reduced. All images were captured immediately before (pre-bleach), immediately after (post-bleach) and at times after photobleaching in the white box. Scale bar: 10 μm . Right: D_{eff} values from FRAP analysis in individual cells. B) Mean values \pm SEM for each condition and variant in 4A. C) Upper panel: D_{eff} values from FRAP analysis in individual Tet-On HD CHO-K1 cells treated with or without dox for 48h and transiently co-transfected with both ER-RFP and CytERM msfGFP membrane reporter. Lower panel: Mean \pm SEM for each condition and construct. *** $p < 0.0001$ in a two-tailed Student t test.

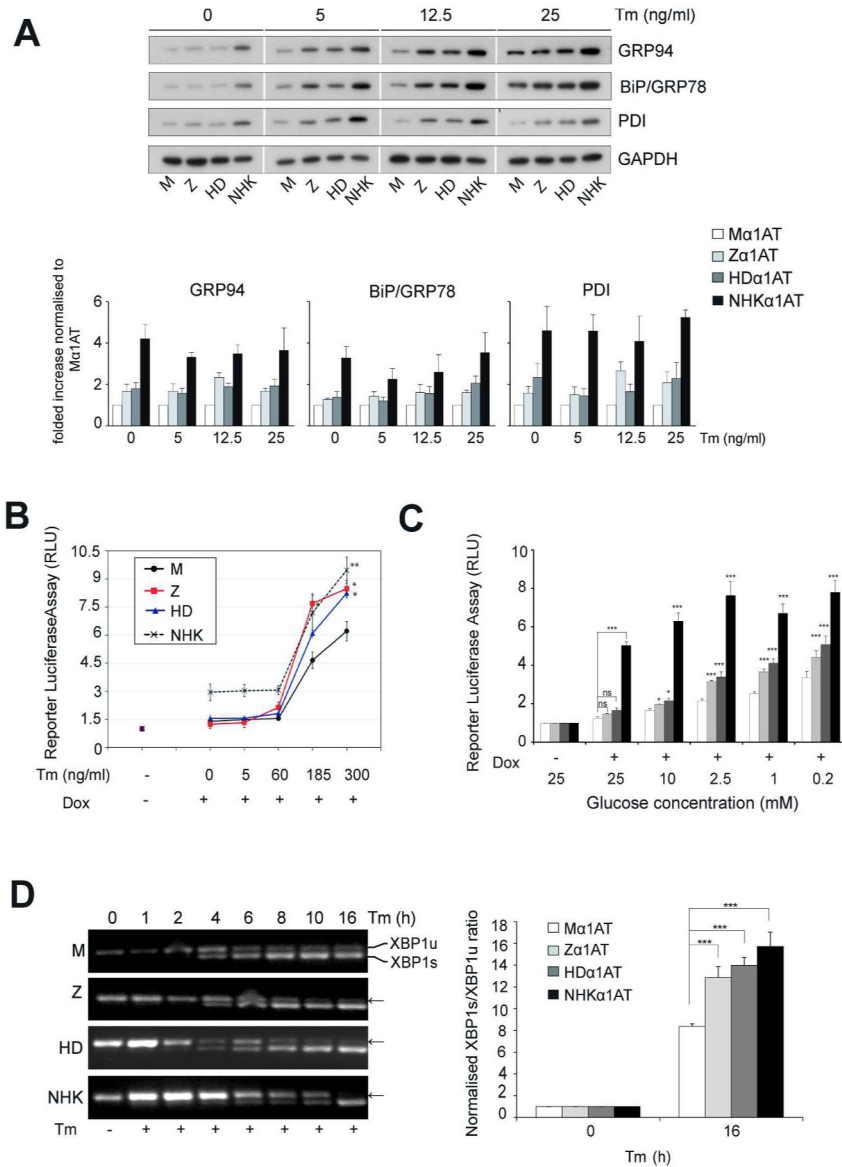


Fig. 5. Differential activation of three UPR sensors in polymeric forms of α_1 -antitrypsin reveals an increased sensitivity to UPR following a second hit

A) Immunoblot of whole cells lysates from CHO-K1 Tet-On cells induced with dox for 48h and treated with the indicated doses of tunicamycin (Tm) for 16h. Grouping of separated lanes within the same gel was performed and indicated by dividing white lines. Histogram representation of four independent replicates of experiment 5A showing fold increase of GRP94, BiP/GRP78 or PDI normalised to loading control and then to wildtype variant for each concentration of tunicamycin (mean \pm SEM). B and C) ATF6 activation during induction of ER stress. α_1 -Antitrypsin expression was induced with dox for 48h. Twenty-four hours prior to lysis, the cells were co-transfected for 6h with a p5xATF6-Luc encoding firefly luciferase under the control of a UPR response element and with pRL-TK *Renilla* luciferase as a normalization control, and then treated with the indicated doses of tunicamycin (B) or glucose (C) for 16h. The graphs show firefly luciferase normalised to *Renilla* luciferase, as mean \pm SEM (n=3). C) *XBP1* processing during ER stress induction. Cells were induced with dox for 48h and subjected to a time course of tunicamycin

treatment (300 ng/mL). RT-PCR was used to amplify *XBPI* mRNA and PCR products were resolved by 2% w/v agarose gel electrophoresis. The ratio of spliced/unspliced *XBPI* mRNA for each α_1 -antitrypsin variant after 16h tunicamycin is represented graphically as mean \pm SEM (n=3). *p<0.05, **p<0.01, or ***p<0.001 according to ANOVA test followed by a Bonferroni *post hoc* test.

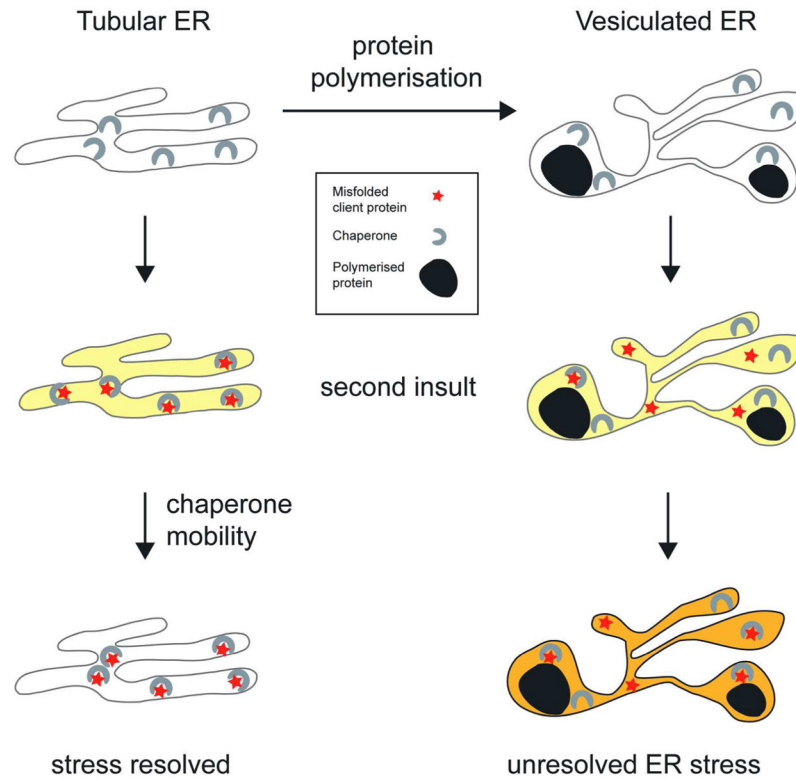


Fig. 6. Model for the enhanced sensitivity to ER stress seen in cells experiencing ER overload
 An insult resulting in misfolded client protein is effectively buffered by chaperone diffusion in healthy cells. This prevents ER stress (“resolved”). In contrast, in cells that accumulate polymerised protein, the global ER environment is affected that impairs chaperone access to misfolded proteins thereby increasing the cell’s propensity to experience ER stress (“unresolved”). Yellow represents a resolved ER stress, while orange corresponds to an unresolved ER response to ER overload.